American Mineralogist, Volume 71, pages 589–598, 1986

Optical studies of biaxial Al-related color centers in smoky quartz

DEBORAH P. PARTLOW,[1] ALVIN J. COHEN
Department of Geology and Planetary Science, University of Pittsburgh
Pittsburgh, Pennsylvania 15260

ABSTRACT

Three optical absorption bands, A_1, A_2, and A_3, are associated with trapped hole centers that develop when quartz containing Al^{3+} in a substitutional Si^{4+} site is subjected to ionizing radiation. Studies of the directional anisotropy of the A_2 and A_3 optical bands in the quartz basal plane show that they may interchange orientations from crystal to crystal in major rhombohedral growth; this contradicts an earlier theory that the anisotropy results from site selectivity of Al^{3+} occurring only in minor rhombohedral growth. Four crystallographic directions have been found for the maximum intensity of A_2 and/or A_3: $[0\bar{1}10]$, $[\bar{1}\bar{3}40]$, $[\bar{1}\bar{1}20]$, and $[\bar{1}\bar{4}50]$. The removal of basal-plane anisotropy at ~500°C reported by others was confirmed and is attributed to the homogenization of interstitial atoms providing charge compensation for substitutional Al^{3+}.

Thermal bleaching studies were conducted to investigate relationships among the A bands and to observe their association with the B band, which is related to a trapped-electron center. A plot of the Nf (product of number of absorbing centers times oscillator strength) for the A_2 band vs. the B band with bleaching temperature forms a straight line with a slope ~1.0, which is identical to a comparable plot of the growth of the analogous H_2^+ and E_3^- bands studied earlier in soda silica glass. This strengthens the model that the center responsible for B is the trapped-electron analogue of trapped-hole center responsible for A_2.

Plots of Nf for A_3 vs. A_1, A_3 vs. A_2, and A_2 vs. A_1 with bleaching temperature all form straight lines, suggesting a close relationship among the centers related to these optical bands. Since the center related to A_3 is known to involve a single trapped hole, it is concluded that all of these centers involve only one trapped hole.

INTRODUCTION

The beginning of our present understanding of the color centers associated with the smoky color that develops in most α-quartz upon exposure to ionizing radiation was the discovery of an EPR signal whose intensity was related to the intensity of the optical absorption in these samples and the suggestion that the centers involved some foreign atom, most probably ^{27}Al (Griffiths et al., 1954). A theoretical interpretation soon followed (O'Brien, 1955), yielding a model that placed the Al atom at a substitutional Si site in the lattice, with a hole trapped in a nonbonding orbital on one of the nearest oxygens. It was also stated that the four O atoms located at the corners of a tetrahedron surrounding the Si site actually formed two nonequivalent pairs and that only one pair was suitable for formation of this center. This was later confirmed by the EPR work of Schnadt and Schneider (1970), who concluded that these suitable oxygens were slightly closer to the Si than the remaining pair. The equivalency of these oxygens was supported by the discovery of thermally activated hopping of the spin among the equivalent O sites in crystalline quartz; this effect was not found in fused silica, because local distortions make all four O sites nonequivalent (Schnadt and Räuber, 1971). A recent report by Nuttall and Weil (1981) shows EPR evidence that the trapping oxygens are actually the pair located farther from the Si site.

Mitchell and Paige (1954) found optical absorption bands that they also associated with the smoky color of irradiated quartz. These bands, A_1 (2.0 eV) and A_2 (~2.7 eV), were assigned to forbidden and allowed electronic transitions by O'Brien (1955). Optical spectroscopy done in polarized light showed that the A_1 and A_2 bands displayed anisotropy in the optic plane corresponding exactly with the crystallographic axes of the quartz structure (Cohen, 1956). This, together with the fact that the Al content of the specimens correlated with the absorption intensities, provided conclusive evidence that these absorption bands were indeed associated with substitutional Al. EPR work (Mackey et al., 1970) showed that the center modeled by O'Brien could include an interstitial monovalent ion (H^+, Na^+, or Li^+) adjacent to the substitutional Al.

Nassau and Prescott (1975) irradiated and heat treated over 300 natural and synthetic quartz samples and found

[1] Present address: Westinghouse R&D Center, 1310 Beulah Road, Pittsburgh, Pennsylvania 15235.

0003–004X/86/0304–0589$02.00

Table 1. Emission analyses of quartz crystals (atoms per 10^6 Si atoms)*

Element	Sample X542-3[1]	Brazilian quartz[2]	R-27[3]	R-27**	B-4[4]
Al	734	222	445	734	156
B	278	NF	ND	ND	NF
Ca	49	NF	ND	ND	NF
Fe	54	NF	27	22	NF
Ge	NF	NF	579	598	NF
Li	285	87	865	727	NF
Mg	25	NF	ND	ND	NF
Na	NF	NF	NF	NF	NF
Ti	38	NF	NF	NF	NF

*actual values believed to lie between 1/3 and 3 times values indicated. NF = not found; element below detection level. ND = not done; no analysis performed for that element.
**D.C. plasma arc analysis done to confirm emission spectroscopic method.

1. Major rhombohedral growth, courtesy K. Nassau, Bell Telephone Laboratories, Murray Hill, N.J.
2. Brazilian quartz, courtesy E.W.J. Mitchell, Clarendon Laboratory, Oxford University.
3. Rhombohedral growth, courtesy the late G. T. Kohman, Bell Telephone Laboratories.
4. Rhombohedral growth, courtesy J. M. Stanley, Signal Corps Engineering Laboratories, Fort Monmouth, N.J.

that the optical absorption spectra of some of these quartzes showed the A_1 and A_2 bands, but the samples showed no smoky color. This corroborated the earlier finding that the EPR and optical spectra did not always correlate directly (Mackey, 1963). However, upon further irradiation of these unusual samples, the development of smoky color was accompanied by the appearance of the EPR signal assigned to the Al-trapped hole center and by the appearance of a previously unrecognized optical absorption band at 2.9 eV, which was designated A_3. This discovery opened the door to the most recent models for the trapped-hole color centers associated with substitutional Al in quartz (Cohen and Makar, 1982). These models suggest that the A_1 band is related to a center consisting of three nonbonded oxygens attached to the Al, with a trapped hole related to them; A_2 is analogous, but only two nonbonded oxygens are present; and only one nonbonded oxygen is attached to the Al in the center associated with A_3. This is supported by the observation that only H_2^+ and H_3^+ absorption bands are seen in soda silica glasses ($Na_2O \cdot 3SiO_2$). These bands are analogous to the A_2 and A_1 quartz bands, respectively, in terms of peak energy and width at half maximum. The high soda content of the glasses precludes the presence of an analogue to A_3.

Nuttall and Weil (1981) presented an important review of the magnetic properties of the O-hole Al centers in quartz. They designated the center responsible for the A_3 optical band as $[AlO_4]^0$. Weil (1975, 1984) has reviewed the literature to 1975 concerning the Al centers in α-quartz and to 1984 concerning the EPR of defects in quartz in general. These two review papers provide excellent references to the literature on this subject.

An additional finding of importance to this work is the anomalous pleochroism observed by Tsinober et al. (1967) in basal-plane sections of smoky synthetic quartz of minor rhombohedral growth, which they attributed to a nonrandom Al occupancy of Si sites that differed on opposite sides of the seed plate. This effect was confirmed by Nassau and Prescott (1978) for the A_3 band, while the other A bands did not differ on opposite sides of the seed. They also felt that site selectivity of Al ions, possibly accompanied by charge compensators, was responsible. The present work gives a different explanation for the anomalous pleochroism of the Al-trapped hole centers in the basal plane of rhombohedral growth synthetic quartz.

Experimental methods

The samples

Four single crystals of α-quartz were used in this work. Their sources, growth orientation, and chemical analyses are given in Table 1. Using an optical interference technique (Nuttall and Weil, 1981), sample R-27 was found to be left-handed, while the other three crystals were right-handed. Two samples, X542-3 and the Brazilian crystal, were used for bleaching studies.

Sample X542-3 had previously been γ-irradiated to saturation and heated incrementally to 280°C, which had produced a definite blue color in the quartz (Nassau and Prescott, 1977). This coloration was, however, quite uneven, and swirled patterns of deeper and paler color became more evident when the slices of this sample were re-irradiated to the smoky condition. Therefore, a 3-mm area of fairly uniform color was selected in each slice for optical measurements. Chemical analysis was done on the uniform area from the slice cut parallel to $(10\bar{1}0)$; the uniform area on the (0001) slice was slightly darker in color and was not analyzed. The Brazilian quartz had been previously X-irradiated, showing pale smoky color. It was re-irradiated using ^{60}Co γ-irradiation to optical saturation of the absorption spectrum in order to carry out bleaching studies. After this treatment, slices of the sample were very uniform in color except for narrow darker bands that could easily be avoided in the optical measurements.

Sample R-27 had also been previously X-irradiated. Thus it was given a smaller γ-ray dose because of its already high optical density. While one region of this sample remained colorless, the smoky area was quite uniform.

Sample B-4 was the only quartz received as a whole untreated colorless crystal. Upon γ-irradiation it took on a banded or striped appearance of light and dark smoky regions only fractions of a millimeter wide. A 3-mm-wide group of dark bands was selected for optical measurements and chemical analysis.

Sample preparation

All samples were crystallographically oriented using a standard back-reflection Laue method (Wood, 1963). A diamond saw blade of thickness 0.175 mm was used to cut slices parallel to (0001) and $(10\bar{1}0)$, except for sample B-4, where the latter slice was cut parallel to $(1\bar{2}10)$. For each sample, both slices were waxed onto a flat polishing block and given a final polish with 0.3-μm ceria polishing compound, so that both slices had the same thickness. The measured sample thicknesses were X542-3, 0.1445 cm; Brazilian quartz, 0.1735 cm; R-27, 0.1590 cm; and B-4, 0.1430 cm.

Gamma irradiation was done in a ^{60}Co cell, and estimated doses were calculated from a measurement of the dose rate of 4.8×10^5 rads per hour, using a Victoreen Radacon III, model 550-1-5, equipped with a 550-6-25 probe. The estimated doses were X542-3 and Brazilian quartz, both 138 megarads; R-27, 0.36 megarads; B-4, 115 megarads.

Table 2. Absorption band peaks and widths at half maximum ($W_{1/2}$) for Al-trapped hole and B centers in α-quartz [values in electron volts (eV)]

Specimen and Orientation	A_1		A_2		A_3		B	
	absorption band peak	$W_{1/2}$	absorption band peak	$W_{1/2}$	absorption band peak	$W_{1/2}$	absorption band peak	$W_{1/2}$
Bell Synthetic Quartz no. X542-3 major rhombohedral growth								
slice cut along $(10\bar{1}0)$								
E ∥ [0001] (π)	1.83	0.65	2.55	0.85	3.00	1.55	3.98	1.30
E ∥ $[1\bar{2}10]$ (σ)[1]	1.85	0.66	2.45	0.87	3.03	1.54	3.92	1.20
normal light	1.84	0.65	2.51	0.86	3.01	1.55	3.95	1.25
slice cut along (0001)								
E ∥ $[0\bar{1}10]$ (A_2 max)[2]			2.40	0.85			3.85	1.20
E ∥ $[2\bar{1}\bar{1}0]$ (A_2 min)[3]			2.44	0.87			3.92	1.25
after 500°C E ∥ $[\bar{1}\bar{3}40]$ (A_3 max)[4]					3.03	1.40	3.88	1.15
after 500°C E ∥ $[43\bar{1}0]$ (A_3 min)[5]					3.00	1.40	3.97	1.15
before heating normal light	1.82	0.71	2.42	0.86	3.06	1.55	3.89	1.23
after 500°C normal light	1.81	0.68	2.38	0.85	3.02	1.40	3.92	1.15
U.S. Army Signal Corps. Synthetic Quartz no. B-4 rhombohedral growth								
slice cut along (0001)								
E ∥ $[\bar{1}\bar{3}40]$ (A_2 max)[4]			2.43	0.83			3.97	1.18
E ∥ $[43\bar{1}0]$ (A_2 min)[5]			2.40	0.82			3.97	1.15
E ∥ $[\bar{1}\bar{1}20]$ (A_3 max)[6]					3.02	1.43	3.95	1.20
E ∥ $[1\bar{1}00]$ (A_3 min)[7]					3.00	1.45	3.95	1.18
normal light	1.84	0.69	2.41	0.83	3.00	1.43	3.96	1.18
Bell Synthetic Quartz no. R-27 rhombohedral growth								
slice cut along (0001)								
E ∥ $[\bar{1}\bar{1}20]$ (A_2 max)[6]			2.43	0.81			3.97	1.20
E ∥ $[1\bar{1}00]$ (A_2 min)[7]			2.42	0.83			3.92	1.18
E ∥ $[\bar{1}450]$ (A_3 max)[8]					2.95	1.44	3.92	1.22
E ∥ $[54\bar{1}0]$ (A_3 min)[9]					2.93	1.40	3.93	1.22
normal light	1.85	0.67	2.42	0.82	2.96	1.41	3.93	1.20
Brazilian Quartz								
slice cut along $(10\bar{1}0)$								
E ∥ [0001] (π)	1.77	0.60	2.60	0.83	3.02	1.53	3.97	1.28
E ∥ $[1\bar{2}10]$ (σ)[1]	1.88	0.60	2.55	0.87	3.03	1.53	3.97	1.27
normal light	1.81	0.60	2.58	0.84	3.02	1.53	3.97	1.28

1. Electric vector (E) ∥ to a_2 axis.
2. E ⊥ to a_1 axis.
3. E ∥ to a_1 axis.
4. E -44° from a_2 axis.
5. E +46° from a_2 axis.
6. E ∥ to a_3 axis.
7. E ⊥ to a_3 axis.
8. E -41° from a_2 axis.
9. E +49° from a_2 axis.

Thermal bleaching was done by heating the sample in a Fisher Programmable Ashing Furnace, model 495, in air. To prevent contamination of the crystal during heating, it was cleaned prior to each bleaching step with pure dry ethanol. It was also placed on a slab of pure, UV-grade fused silica (Corning 7940) during heating. Temperature was monitored with a chromel-alumel thermocouple, with the bead placed on the glass slab about 1 mm from the crystal. The heating rate used for this work was 5°C/min, and the time at the designated temperature was 2 h. For the Brazilian quartz, 25° heating increments were used up to 325°C. Thereafter, 50° increments were required to produce noticeable decreases in spectral absorption. For X542-3 quartz, the initial 20° increments were cut to 10° because of the rapid bleaching observed in the range 200 to 240°C. In the range 240 to 300°C, 20° increments were appropriate, and this was raised to 40° until 460°C, after which no changes were observed.

Spectrophotometric studies

Optical measurements were done at room temperature on a Varian model 2300 spectrophotometer, which is a double-beam instrument equipped with a computer for data storage and reduction. Polarization of the beam was accomplished using a UV-grade quartz Rochon prism, which was mounted in the entrance wall to the sample compartment such that it could be reproducibly rotated in 15° increments. Although both the extraordinary (e) and ordinary (o) rays are transmitted by this type of prism, the 3-mm aperture used for the sample was sufficiently small that the e ray was excluded from the light path. The sample holder was modified so that the same optical area of the sample could be maintained after each thermal bleaching treatment. Crystal orientation was preserved through the use of inscribed guide marks. Although the sample could be rotated in any increment

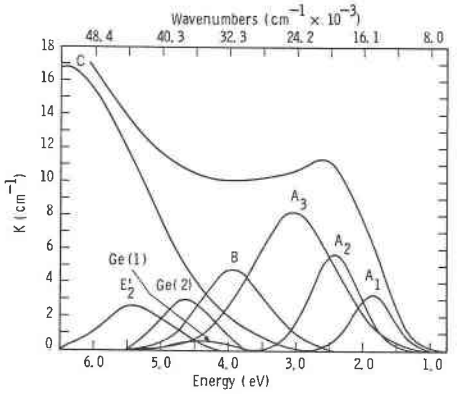

Fig. 1. Gaussian resolution of the spectrum of sample X542-3 after spectral saturation using γ-irradiation. Data recorded with light polarized along [1$\bar{2}$10] in the slice parallel to (10$\bar{1}$0).

because of its kinematic mount, sample rotation was done only for the Brazilian crystal. For the other samples, the sample was held stationary and the polarizer was rotated, primarily because of the unevenness of the smoky color in samples X542-3 and B-4. Although sample R-27 was uniformly colored, it was held stationary so that anisotropy measurements were all done by the same method. Normal light refers to light having only the internal polarization of the instrument, without additional deliberate polarization.

Data reduction

Resolution of the spectra into gaussian components was done using a DuPont 310 curve analyzer. Thermal bleaching data were taken from difference spectra, which were calculated by subtracting the spectrum of the bleached sample from that of the sample after optical saturation using γ-irradiation.

The product Nf (number of absorbing centers times the oscillator strength per cubic centimeter) was calculated using the modified Smakula equation of Lax (1955, p. 127) and Dexter (1956, p. 52).

Results and discussion

Spectra of each of the four crystals studied were recorded after γ-irradiation using normal light and using light polarized along various crystal directions, as summarized in Table 2. Figure 1 illustrates the resolution of one of these spectra into gaussian components. The absorption-peak positions and widths at half-maximum ($W_{1/2}$) determined by such resolution are given in Table 2 for the bands of primary interest here—A_1, A_2, A_3, and B—and are in good agreement with those found by Nassau and Prescott (1975). These bands are discussed in greater detail in the following subsections.

The high-energy region of these spectra, i.e., above 4.0 eV, is quite complex. For the present work, five bands were used for resolution in this region. The "C" band, located anywhere between 5.8 (Mitchell and Paige, 1954) and 6.4 eV, is composed of several bands, including the E'_1 band. The E'_1 and E'_2 centers, with absorption bands in quartz at 5.85 and 5.40 eV, respectively, have been identified by EPR as trapped-electron centers (Weeks, 1963; Weeks and Lell, 1964). A recent model for the E'_1 center is the "relaxed O^- vacancy" model, where an O atom and an additional electron are removed, and the unpaired electron spends most of its time on one of the two adjacent silicons (Gobsch et al., 1978). The E'_2 center is thought to be an Si–O vacancy with an electron trapped on the defect Si from which the O is missing (Weeks, 1963). In order to obtain acceptable approximations of the experimental curves, it was necessary to include at least one of two bands at 4.28 and at 4.5–5.0 eV that are due to trapped-electron centers associated with Ge impurity in quartz (Cohen and Smith, 1958; Anderson and Weil, 1959; Wright et al., 1963; Halperin and Ralph, 1963). Although R-27 is the only sample shown by chemical analysis to contain Ge in appreciable amounts, traces of Ge are most likely present in all SiO_2 derived from natural quartz (Cohen, 1959).

Difference spectra for each bleaching temperature for Bell X542-3 and for the Brazilian quartz, totaling 66 individual spectra, were also resolved as shown in Figure 1. These spectra had been recorded using light polarized with the electric vector parallel to [0001] and [1$\bar{2}$10] in the slice cut along (10$\bar{1}$0). For the X542-3 quartz, spectra were also recorded in the directions of maximum and minimum intensity of the A_2 band, [0$\bar{1}$10] and [2$\bar{1}$10], respectively, in the slice cut along (0001). The Brazilian quartz was isotropic in (0001). Plots of Nf versus bleaching temperature for crystal X542-3 are shown in Figure 2 for the A_1, A_2, A_3, and B bands in selected crystallographic directions.

Absorption-band anisotropy in the basal plane

Basal-plane anisotropy (anomalous pleochroism) of various optical absorption bands associated with impurities in quartz has been observed by a number of investigators (Tsinober, 1962; Tsinober et al., 1967; Hassan and Cohen, 1974; Nassau and Prescott, 1978; Cohen and Makar, 1985). Several of these investigators reported that the orientation of maximum intensity for a given optical band was at 90° to that of minimum intensity. Figure 3 illustrates a similar trend for A_2 and A_3 bands in basal-plane sections of three of the crystals studied here. As mentioned above, the Brazilian quartz was isotropic in the basal plane. The curves in Figure 3a and 3d were obtained at 2.5 eV, the peak position for A_2, while those in Figure 3b and 3c were taken at 3.3 eV, which is on the high-energy shoulder of the A_3 band, in order to minimize interference from A_2. Similar measurements were attempted at 1.3 eV, on the low-energy shoulder of A_1, as discussed below. The B band, at 3.95 eV, was found to be isotropic in the basal plane. The orientations of the absorption band maxima shown in Figure 3 were pinpointed by assuming that the bands showing maxima near [0$\bar{1}$10] or [$\bar{1}\bar{1}$20] were actually oriented exactly along those directions, since these orientations have been reported in other studies of impurity-related optical absorption bands in quartz (Tsinober, 1962; Hassan and Cohen, 1974; Cohen and Makar, 1985), and since the quartz structure

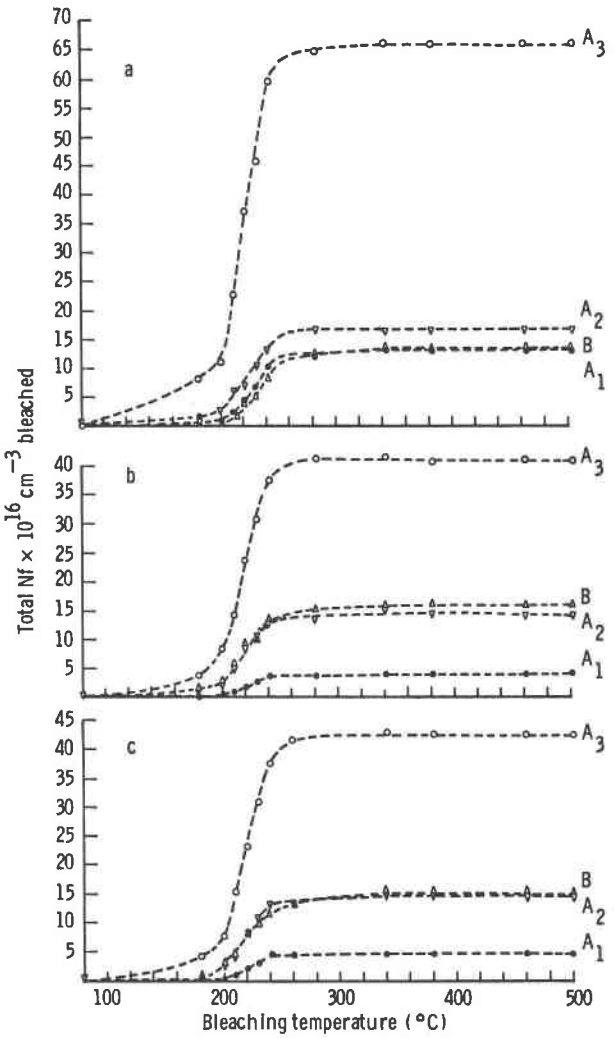

Fig. 2. Product of number of absorbing centers and oscillator strength (Nf) versus thermal bleaching temperature for absorption bands in sample X542-3; spectra recorded using light polarized (a) along [0001] in a slice cut in (10$\bar{1}$0), (b) along [1$\bar{2}$10] in a slice cut in (10$\bar{1}$0), (c) along [0$\bar{1}$10] in a slice cut in (0001). ● 1.85 eV (A_1), ▽ 2.5 eV (A_2), ○ 3.0 eV (A_3), △ 3.95 eV (B).

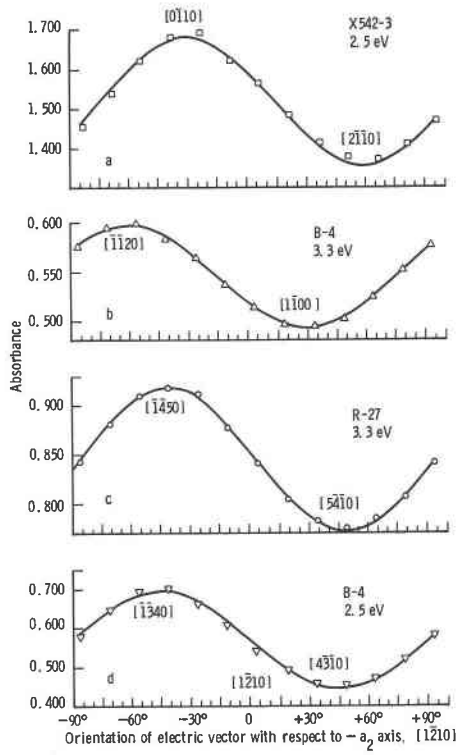

Fig. 3. Absorbance versus orientation of electric vector (E) of light polarized along various directions in the basal plane. □ sample X542-3, 2.5 eV; △ sample B-4, 3.3 eV; ○ sample R-27, 3.3 eV; ▽ sample B-4, 2.5 eV.

contains void channels along those directions that could accommodate impurities. A method of least squares was used to fit each set of experimental data to a sine curve, the maximum error being <2%. Thus the experimental maxima were found by calculation. For each band showing a maximum near [0$\bar{1}$10] or [$\bar{1}\bar{1}$20], the correction factor needed to shift the maximum to that direction was determined. This correction factor was then applied to the experimental maximum for the other band in that sample, in order to determine whether it was oriented along [$\bar{1}\bar{2}$30], [$\bar{1}\bar{4}$50], or [$\bar{1}\bar{3}$40], since these directions are all within 8° of each other. Figure 3 illustrates that a given absorption band may differ in the orientation of its maximum intensity in the basal plane from crystal to crystal. This effect is similar to that observed by Nassau and Prescott (1978) for the A_3 band in basal-plane samples taken from opposite sides of the seed plate, within single synthetic crystals of minor rhombohedral (z) growth. They also reported isotropic behavior for a Brazilian crystal.

However, our findings differ from those of Nassau and Prescott in several ways. While they saw a differing direction in anisotropy for A_3 only, we show this difference for both A_2 and A_3; we were unable to obtain usable data for A_1, because of the overwhelming effect of A_2 in the region of the A_1 gaussian band. The directional ranges reported by Nassau and Prescott for the maximum intensity at various energies do include the directions shown in Table 3 for the bands studied here, and Tsinober et al. (1967) reported a maximum at 480 nm (2.58 eV) along [0$\bar{1}$10], which coincides with the A_2 maximum in sample X542-3. In addition, Nassau and Prescott reported that anomalous pleochroism was found only in quartz of minor rhombohedral growth, while we show that it is clearly present in sample no. X542-3, which was grown on the major rhombohedron (r) (Nassau and Prescott, 1977), in no. R-27, which is also thought to be of r-face growth (Cohen, ms.), and in B-4, which may be of either r- or z-face growth. Furthermore, they reported that the anomalous pleochroism of over 80 crystals of minor rhombohedral growth appeared identical, while we show that in only three crystals there are three different orientations for the maxima of A_2 and A_3.

The explanation given by Nassau and Prescott (1978)

Table 3. Orientation of maximum and minimum absorbance of A_2 and A_3 absorption bands in basal plane (0001) of rhombohedral growth of synthetic α-quartz crystals with respect to the reference direction $[1\bar{2}10]$, $-a_2$

Crystal	A_3		A_2		Remarks
	max.	min.	max.	min.	
Bell quartz no. X542-3	$[\bar{1}\bar{3}40]$	$[4\bar{3}\bar{1}0]$	$[0\bar{1}10]$	$[2\bar{1}\bar{1}0]$	nearly isotropic in basal plane after heating at 500°C for 2 hrs. Grown on r $(10\bar{1}1)$ seed.*
Signal Corps quartz no. B-4	$[\bar{1}\bar{1}20]$	$[1\bar{1}00]$	$[\bar{1}\bar{3}40]$	$[4\bar{3}\bar{1}0]$	not known whether grown on r or z $(01\bar{1}1)$ seed.*
Bell quartz no. R-27 (Ge impurity)	$[\bar{1}\bar{4}50]$	$[5\bar{4}\bar{1}0]$	$[\bar{1}\bar{1}20]$	$[1\bar{1}00]$	probably grown on r seed.*

*no data for A_1 absorption band because of overlap by the A_2 band.

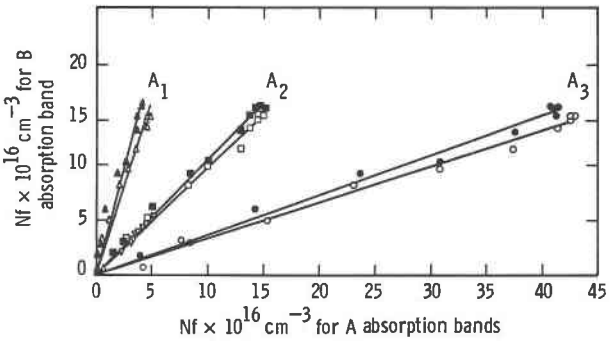

Fig. 4. Plot of Nf for A absorption bands versus Nf for B absorption band for the same bleaching temperature in sample X542-3. Open symbols, slice cut in (0001), light polarized along $[0\bar{1}10]$ (A_2 maximum). Solid symbols, slice cut in $(10\bar{1}0)$ light polarized along $[1\bar{2}10]$. ▽ indicates growth data for the H_2^+ versus the E_3^- absorption bands in soda silica glass ($Na_2O \cdot 3SiO_2$) from Cohen and Janezic (1983, Fig. 3).

for their observations of anomalous pleochroism in z-face growth crystals is that a site selectivity exists for the Al ion due to a difference in the energy of substitution for these ions in differently oriented AlO_4 tetrahedra. They explain that, of the dominant growth surfaces for quartz, i.e., prism faces, rhombohedral faces, and basal surface, only the minor rhombohedral face shows a strong preferential presentation of just one of the symmetrically equivalent tetrahedral sites; thus, by their scenario, only z-face growth quartz can exhibit basal-plane anisotropy of Al-related centers. Our results are therefore in conflict with this scenario.

Nassau and Prescott (1978) observed a loss of anisotropy upon heating quartz at temperatures as low as 490°C for extended periods. Tsinober et al. (1967) had reported this phenomenon at 600°C, noting further that crystals grown at 520–600°C showed no anomalous pleochroism. They all agreed that the effect was due to the mobility of Al ions upon heating, with Nassau and Prescott adding that charge compensators might be involved. We have also seen this loss of pleochroism in the basal plane below 500°C, but feel that it can only be due to migration of interstitial charge compensators, since the breaking of covalent Al–O bonds, a disruption of the quartz structure, cannot occur at such low temperatures (Cohen, 1975; Cohen and Makar, 1982).

Table 3, which summarizes our findings for the orientations of maximum and minimum intensity for the A_2 and A_3 bands, shows a total of six cases involving four different orientations and implies 48 possible combinations, considering the three different Al^{3+} sites in the basal plane (Taylor and Farnell, 1964), excluding any distinction between right- and left-handed quartz. If A_1 shows similar behavior, which we could not determine experimentally, then there would be 192 combinations. While only four directions of maximum A-band intensity were found here—$[\bar{1}\bar{1}20]$, $[0\bar{1}10]$, $[\bar{1}\bar{3}40]$, and $[\bar{1}\bar{4}50]$—further research is needed to see whether other directions such as $[\bar{5}\bar{1}60]$, $[\bar{1}\bar{2}30]$, and $[\bar{2}\bar{3}50]$ are also intensity maximum directions. In a study of the basal-plane biaxiality of color-center absorption bands in amethyst quartz, Hassan and Cohen (1974) found absorption maxima in $[\bar{1}\bar{1}20]$, $[0\bar{1}10]$, $[\bar{1}\bar{2}30]$, and $[\bar{1}\bar{4}50]$. One of these directions, $[\bar{1}\bar{2}30]$, has not as yet been reported for the A_2 or A_3 band maxima in smoky quartz but is thus likely to occur. These limited data indicate that the A optical absorption bands interchange their orientations in at least four directions in different rhombohedral growth smoky quartz crystals. These orientation directions must be related to the unequal distribution of charge compensators for substitutional Al upon growth which later homogenize upon heating to $\gtrsim$500°C. In addition, the nonbonding oxygens (to silicons) in the models proposed by Cohen and Makar (1982) may be bonded to interstitial charge compensators such as Fe and Ti. The orientation directions lying along $[\bar{1}\bar{3}40]$ and $[\bar{1}\bar{4}50]$ could be related to interstitials in voids that are not in the basal plane.

B absorption band and trapped-electron model

The B absorption band was seen in fused silica (Mitchell and Paige, 1954) and later in quartz (Nassau and Prescott, 1975) at approximately 4.0 eV, with a $W_{1/2}$ of ~1.2 eV. It was pointed out by Cohen and Makar (1982) that this band is analogous to the E_3^- band found by Mackey et al. (1966) in soda silica glass near 4.0 eV with a $W_{1/2}$ of 1.16 eV, which they attributed to a trapped-electron center.

Comparison between *B* and A_2 absorption bands. Cohen and Janezic (1983) showed that the E_3^- and H_2^+ absorption bands in soda silica glass have the same growth behavior upon X-irradiation. Therefore they conclude that E_3^- is the trapped-electron compliment of H_2^+, i.e., E_3^- is related to a trapped-electron center associated with two nonbonded oxygens on a tetrahedron. As has been discussed in the previous sections, the B and A_2 bands in quartz are analogous to E_3^- and H_2^+, respectively, in glass. Mackey et al. (1966) also concluded that E_3^- is related to a trapped-

electron center on the basis of light bleaching experiments on soda silica glass. Cohen and Makar (1982) thus proposed that the model for the center associated with the B absorption band is the same as the model for the center associated with the E_3^- band. The present findings support this reasoning. Figure 4 shows that the Nf is the same for B and A_2 as thermal bleaching proceeds. Growth data from Cohen and Janezic (1983, Fig. 3) for E_3^- vs. H_2^+ in soda silica glass are included for comparison. Thus it appears that the center associated with the A_2 band is quenched by electrons released from the center associated with the B band upon heating.

B and A_1 absorption bands. As illustrated in Figure 2, the B and A_1 absorption bands follow a similar bleaching relationship in the spectra recorded for sample X542-3 along [0001], while bleaching curves recorded along [$1\bar{2}10$] and [$0\bar{1}10$] are lower for A_1 than for B. However, plots of of Nf for A_1 vs. B with bleaching temperature in these latter two directions do form straight lines with similar slopes as shown in Figure 4, offering evidence of a close relationship between the centers responsible for A_1 and B. This is discussed further in the section on the sum of the $A_1 + A_2$ bands versus the B band.

B and A_3 absorption bands. Once again, the bleaching curves of Figure 2 show that the B and A_3 bands bleach at approximately the same temperature, although the total Nf bleached differs for the two bands. As with the A_1 and A_2 bands, Figure 4 shows a straight-line bleaching relationship between B and A_3, the slopes of these lines being similar for the spectra recorded along [$1\bar{2}10$] and [$0\bar{1}10$]. As with the A_1 and A_2 bands, this is evidence for a close relationship between the centers responsible for A_3 and B.

A_3 absorption band and *GOW* center

The A_3 absorption band, as discussed in the introduction, is responsible for the smoky color of quartz (Nassau and Prescott, 1975) and is associated with the color center often designated *GOW,* after Griffiths et al. (1954), who first reported its EPR signal. A recent model for this center consists of a substitutional Al surrounded by a tetrahedron of oxygens, only one of these being nonbonded, with a trapped hole related to that one O (Cohen and Makar, 1982).

A_3 band vs. A_2 band. Figure 5a shows that plots for sample X542-3 with the Nf of A_2 versus the Nf of A_3, at the same bleaching temperature, are straight lines. Data points for the [0001] and [$2\bar{1}\bar{1}0$] directions fall along the same line, as do those for the [$1\bar{2}10$] and [$0\bar{1}10$] directions. Although [$2\bar{1}\bar{1}0$] and [$0\bar{1}10$] are not the directions of maximum and minimum intensity for A_3, they bleach with the actual maxima and minima because they are adjacent to these points on the sine curve of intensity vs. orientation (Fig. 3). The straight-line relationships shown for A_3 vs. A_2 in Figure 5a together with the fact that they interchange orientations in the basal plane indicates a direct relationship between the bands responsible for these centers. Furthermore, the center responsible for A_3 is known

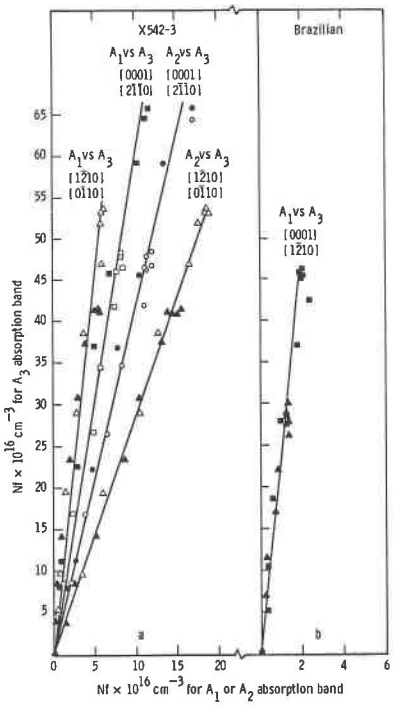

Fig. 5. Plot of Nf for A_1 and A_2 absorption bands versus Nf for A_3 absorption band for the same bleaching temperature in two quartz samples. Slice cut in (0001): □ and ○ indicate polarization along [$2\bar{1}\bar{1}0$]; △ indicates polarization along [$0\bar{1}10$]. Slice cut in ($10\bar{1}0$): ■ and ● indicate polarization along [0001]; ▲ indicates polarization along [$1\bar{2}10$].

to contain a single trapped hole. This supports the suggestion by Cohen and Makar (1982) that these centers are both related to a single trapped hole.

A_3 band vs. A_1 band. Figure 5a shows the same behavior for A_3 vs. A_1 as was outlined above for A_3 vs. A_2, i.e., that data points representing Nf of A_3 vs. Nf of A_1 with bleaching temperature lie along the same straight line for the [0001] and [$2\bar{1}\bar{1}0$] directions in sample X542-3, while points for the [$1\bar{2}10$] and [$0\bar{1}10$] directions lie on a straight line with a different slope. Figure 5b shows that these directions are not the same for the Brazilian quartz, where data points for [0001] and [$1\bar{2}10$] form a single straight line. The trends shown in Figures 5a and 5b suggest that A_1 is related to a single trapped hole because of its close relationship with A_3, as reasoned above for the A_2 band.

A_1 and A_2 absorption bands

Figure 6 shows the same directional similarity for A_1 vs. A_2 as was shown in Figure 5 for each of these bands vs. A_3. Again, data points of Nf for A_1 vs. A_2 with temperature for the [0001] and [$2\bar{1}\bar{1}0$] directions form one straight line, while those for [$1\bar{2}10$] and [$0\bar{1}10$] form another, although the slopes of these lines do not coincide with those of Figure 5. This straight-line relationship may be viewed in conjunction with the observation by Mackey et al. (1966, Fig. 11) of the behavior of comparable H^+ centers in soda silica glass that are believed to contain a

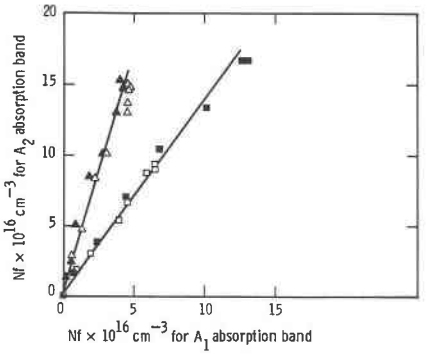

Fig. 6. Plots of Nf for A_1 absorption band versus Nf for A_2 band for the same bleaching temperature in sample X542-3. Slice cut in (0001): △ indicates polarization along [0$\bar{1}$10]; □ indicates polarization along [2$\bar{1}\bar{1}$0]. Slice cut in (10$\bar{1}$0): ▲ indicates polarization along [1$\bar{2}$10]; ■ indicates polarization along [0001].

single trapped hole (Schreurs, 1967). They found that H_2^+ was partially converted to H_3^+ upon low-temperature bleaching with a tungsten lamp. Thus, the lamp furnished the energy to allow the trapped hole to migrate from the H_2^+ center to a precursor of the H_3^+ center, a phenomenon that can only occur between structurally related centers. The close relationship between A_1 and A_2 demonstrated in Figure 6 and the analogy with the H^+ centers of glass

Table 4. Dichroic ratios for absorption band peaks after optical saturation using γ-irradiation

Specimen and absorption band	K_{max}/K_{min} in (0001)	π/σ[1] in (10$\bar{1}$0)
Bell quartz no. X542-3		
A_1	1.13[2]	2.25
A_2	1.23	1.44
A_3	1.10[2]	1.38
B	1.00	1.16
Signal Corps quartz no. B-4		
A_1	1.04	
A_2	1.55	
A_3	1.20	
B	1.04	
Bell quartz no. R-27		
A_1	1.08	
A_2	1.53	
A_3	1.18	
B	1.03	
Brazilian Quartz		
A_1		2.00
A_2		1.53
A_3		1.05
B		1.27
Bell quartz no. LC 3237-15[3]		
A_3 (3.0 eV) l	1.15	
u	1.22	
B (4.0 eV) l	<1.03	
u	1.08	

1. π = E∥ [0001]; σ = E∥ [1$\bar{2}$10]
2. data recorded upon re-irradiation with γ-rays after anisotropy was greatly reduced by heating.
3. data from Nassau and Prescott (1978), Table 1) l and u indicate the lower and upper growth directions from the seed plate.

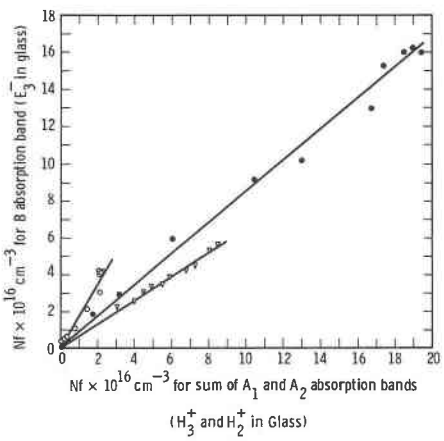

Fig. 7. Plots of Nf for the sum of the $A_1 + A_2$ absorption bands versus Nf for B absorption band for the same bleaching temperature in quartz crystals cut in (10$\bar{1}$0), with light polarized along [1$\bar{2}$10]. ● Bell quartz X542-3. ○ Brazilian quartz. ▽ Similar plot for the growth of analogous absorption bands in soda silica glass (from Cohen and Janezic, 1983, Fig. 11).

again suggests that the A_1 and A_2 bands are each associated with centers involving a single trapped hole.

In a recent paper, Meyer et al. (1984) reported an optical absorption band at 1.96 eV superimposed on the A_1 absorption band. However, close examination of their Figure 3 shows that the sum of the resolved gaussian bands does not match their experimental spectral curve at all energies. In addition, if this resolution of the A absorption bands were used in our work, the agreement in our Figure 4 between the B absorption bands in the quartz would not match the data for the similar centers in soda silica glass, as the $W_{1/2}$ for A_2 in their work, 0.57 ± 0.05, is much smaller than in our work (Table 2). It seems more likely that their second optical transition at 1.96 eV is actually the A_1 band rather than a separate band. Their suggested model for this transition, "a charge transfer transition of the hole from ion O^- adjacent to Al^{3+} to an O^{2-} ion in the next shell," is not far different from the model suggested by Cohen and Makar (1982) for the center associated with the A_1 absorption band.

Sum of $A_1 + A_2$ absorption bands vs. the B absorption band. Figure 7 shows a plot of Nf with bleaching temperature for the sum of the $A_1 + A_2$ bands vs. the B band, for selected directions in sample X542-3 and in the Brazilian quartz. A plot of the analogous bands for soda silica glass was made using growth data from Cohen and Janezic (1983, Fig. 2) and is included for comparison. These three plots are all straight lines of different slopes. The close relationship between the A_1 and A_2 bands is once again underscored. The conversion of the soda silica glass equivalent of the A_2 band to that of the A_1 band mentioned above and the straight-line relationships shown in Figure 7 suggest that the trapped-hole centers associated with both the A_1 and A_2 bands are quenched by electrons released from the trapped-electron center associated with the B band upon heating.

Dichroic ratios of the absorption bands

Table 4 gives the dichroic ratios of the A_1, A_2, A_3, and B absorption bands in the basal and optic planes from all available data obtained in this study. Also shown are comparable data for the A_3 and B bands reported by Nassau and Prescott (1978). Their measurements were made in basal sections of a synthetic quartz crystal in lower and upper seed-plate growth and are in good agreement with our results for these bands.

The dichroism of the A_1 band in $(10\bar{1}0)$ is similar for the two specimens studied. Among the three specimens examined in (0001), the A_3 and A_1 bands each show a fairly consistent dichroic ratio. The B band, as mentioned previously, is essentially isotropic in the basal plane. However, it does show anisotropy in $(10\bar{1}0)$.

In comparing the dichroic ratios in the basal plane and in $(10\bar{1}0)$, the values for A_2 in samples B-4 and R-27 are in good agreement with the A_2 value in the Brazilian quartz. There is less uncertainty in the A_2 dichroic ratios than in those of the other bands listed because of the minimal overlap by the A_3 and A_1 bands in the spectral region where the data are taken. An exceptional case is found in sample X542-3, whose unusually intense A_3 band overlaps significantly with the A_2 band, as shown in Figure 1. Thus the dichroic ratio for A_2 in this sample is not in agreement with those of the other samples.

Conclusions

The orientation of maximum intensity for the A_2 and A_3 optical absorption bands in the basal plane of smoky quartz varies from crystal to crystal. Four orientations were found for A_2 and/or A_3 in three synthetic crystals studied here—$[\bar{1}\bar{1}20]$, $[0\bar{1}10]$, $[\bar{1}\bar{3}40]$, and $[\bar{1}\bar{4}50]$—while the B band was isotropic in the basal plane. The results for A_1 were inconclusive owing to overlap with the A_2 band. A Brazilian quartz showed no basal-plane anisotropy. Since at least one, and probably two, of the synthetic crystals studied were grown on the major rhombohedral face, basal-plane anisotropy does not occur only in minor rhombohedral growth, as proposed by Tsinober et al. (1967) and by Nassau and Prescott (1978). In this work, the anomalous dichroism of the A centers in the basal plane is attibuted to a nonuniform distribution of interstitial ions that provide charge compensation for substitutional Al^{3+} in three nonequivalent sites in this plane.

Thermal bleaching studies show that the relationships among the A_1, A_2, and B bands are very similar to those found for the equivalent bands in growth studies of soda silica glass. These results indicate that the trapped electron-center responsible for the B band is analogous to the trapped-hole center responsible for the A_2 band, i.e., the centers are both associated with a tetrahedron having two nonbonded oxygens. Furthermore, the straight-line plots of the Nf products at the same bleaching temperature for A_1 vs. A_2 vs. A_3, and for A_1 vs. A_3 show a close relationship among the centers related to these bands. Since the center related to A_3 is known to involve only one trapped hole, the results of this work imply that all three of these centers involve only one trapped hole.

Acknowledgments

We wish to thank E. W. J. Mitchell, now of the Clarendon Laboratory, Oxford University; J. M. Stanley of the Signal Corps. Engineering Laboratories, Fort Monmouth, N.J., and the late G. T. Kohman of the Bell Telephone Laboratories, Murray Hill, N.J. for providing quartz crystals used in this work. K. Nassau of the Bell Telephone Laboratories is also thanked, both for providing crystal X542-3 and for efforts to obtain the history of crystal R-27. For his contributions in computer programming and electronics maintenance, we are grateful to W. D. Partlow III of the Westinghouse R&D Center, Pittsburgh, Pennsylvania, where we were allowed access to much of the equipment needed to complete this work.

Richard H. Jahns was promoted to full professor at Cal Tech the year the junior author of this paper was a postdoctoral fellow there in chemistry. Through my need of index of refraction liquids we became acquainted. Twenty years later when we were both invited lecturers at the Geology Department at San Diego State College, on the same day, I finally realized we were actually contemporaries. Whenever I see a large euhedral mineral or a pegmatite, I think of Jahns and how good it was to be with him to share his humor and his sensible views on everything.

References

Anderson, J.H., and Weil, J.A. (1959) Paramagnetic resonance of color centers in germanium-doped quartz. Journal of Chemical Physics, 31, 427–434.

Cohen, A.J. (1956) Anisotropic color centers in α-quartz. Part I. Smoky quartz. Journal of Chemical Physics, 25, 908–914.

——— (1959) The role of germanium impurity in the defect structures of silica and germania. Glastechnische Berichte, 32K, VI/53–VI/58.

——— (1975) On the color centers of iron in amethyst and synthetic quartz: A reply. American Mineralogist, 60, 338–339.

Cohen, A.J., and Janezic, G.G. (1983) Relationships among trapped hole and and trapped electron centers in oxidized soda-silica glasses of high purity. Physica Status Solidi (a), 77, 619–624.

Cohen, A.J., and Makar, L. N. (1982) Models for color centers in smoky quartz. Physica Status Solidi (a), 73, 593–596.

——— (1985) Dynamic biaxial absorption spectra of Ti^{3+} and Fe^{2+} in a natural rose quartz crystal. Mineralogical Magazine, 49, 709–715.

Cohen, A.J., and Smith, H.L. (1958) Anisotropic color centers in α-quartz II germanium-doped synthetic quartz. Journal of Chemical Physics, 28, 401–405.

Dexter, D.L. (1956) Absorption of light by atoms in solids. Physical Review, Series 2, 101, 48–55.

Gobsch, G., Haberlandt, H., Weckner, H.J., and Reinhold, J. (1978) Calculation of the g-tensor and ^{29}Si hyperfine tensors of the E_1' centre in silicon dioxide. Physica Status Solidi (b), 90, 309–317.

Griffiths, J.H.E., Owen, J., and Ward, I.M. (1954) Paramagnetic resonance in neutron-irradiated diamond and smoky quartz. Nature, 173, 439–440.

Halperin, Abraham, and Ralph, J.E. (1963) Optical studies of anisotropic color centers in germanium-doped quartz. Journal of Chemical Physics, 39, 63–73.

Hassan, Farkhonda, and Cohen, A.J. (1974) Biaxial color centers in amethyst quartz. American Mineralogist, 59, 709–718.

Lax, Melvin. (1955) The influence of lattice vibrations on electronic transitions in solids. Photoconductivity Conference, 1954, 111–145. Wiley, New York.

Mackey, J.H., Jr. (1963) An EPR study of impurity related color

centers in germanium-doped quartz. Journal of Chemical Physics, 39, 74–83.
Mackey, J.H., Smith, H.L., and Halperin, A. (1966) Optical studies in x-irradiated high purity sodium silicate glasses. Journal of Physics and Chemistry of Solids, 27, 1759–1772.
Mackey, J.H., Jr., Boss, J.W., and Wood, D.E. (1970) EPR study of substitutional-aluminum-related hole centers in synthetic α-quartz. Journal of Magnetic Resonance, 3, 44–54.
Meyer, B.K., Lohse, F., Spaeth, J.M., and Weil, J.A. (1984) Optically detected magnetic resonance of the $[AlO_4]^0$ centre in crystalline quartz. Journal of Physics C: Solid State Physics, 17, L31–L36.
Mitchell, E.W.J., and Paige, E.G.S. (1954) On the formation of colour centres in quartz. Royal Society of London Proceedings, 67B, 262–264.
Nassau, Kurt, and Prescott, B.E. (1975) A reinterpretation of smoky quartz. Physica Status Solidi (a), 29, 659–663.
——— (1977) Smoky, blue, greenish yellow, and other irradiation-related colors in quartz. Mineralogical Magazine, 41, 301–312.
——— (1978) Growth-induced radiation-developed pleochroic anisotropy in smoky quartz. American Mineralogist, 63, 230–238.
Nuttall, R.H.D., and Weil, J.A. (1981) The magnetic properties of the oxygen-hole aluminum centers in crystalline SiO_2. I. $[AlO_4]^0$. Canadian Journal of Physics, 59, 1696–1708.
O'Brien, M.C.M. (1955) The structure of the colour centres in smoky quartz. Royal Society of London Proceedings, 231A, 404–441.
Schnadt, R., and Räuber, A. (1971) Motional effects in the trapped-hole center in smoky quartz. Solid State Communications, 9, 159–161.
Schnadt, R., and Schneider, J. (1970) The electronic structure of the trapped-hole center in smoky quartz. Physik der kondensierten Materie, 11, 19–42.
Schreurs, J.W.H. (1967) Study of some trapped hole centers in x-irradiated alkali silicate glasses. Journal of Chemical Physics, 47, 818–830.
Taylor, A.L., and Farnell, G.W. (1964) Spin-lattice interaction experiments on color centers in quartz. Canadian Journal of Physics, 42, 595–607.
Tsinober, L.I. (1962) A feature of the pleochroism of colored synthetic quartz. Soviet Physics—Crystallography, 7, 113–114.
Tsinober, L.I., Samoilovich, M.I., Gordienko, L.A., and Chentsova, L.G. (1967) Anomalous pleochroism in synthetic smoky quartz crystals. Soviet Physics—Crystallography, 12, 53–56.
Weeks, R.A. (1963) Paramagnetic spectra of E_2' centers in crystalline quartz. Physical Review, 130, 570–576.
Weeks, R.A., and Lell, E. (1964) Relation between E′ centers and hydroxyl bonds in silica. Journal of Applied Physics, 35, 1932–1938.
Weil, J.A. (1975) The aluminum centers in α-quartz. Radiation Effects, 26, 261–265.
——— (1984) A review of electron spin spectroscopy and its application to the study of paramagnetic defects in crystalline quartz. Physics and Chemistry of Minerals, 10, 149–165.
Wood, E.A. (1963) How to take back reflection photographs. In Crystal Orientation Manual, 28–29. Columbia University Press, New York.
Wright, P.M., Weil, J.A., Buch, T., and Anderson, J.H. (1963) Titanium colour centers in rose quartz. Nature, 197, 246–248.

Manuscript received May 14, 1985
Manuscript accepted November 17, 1985